Polymer 55 (2014) 5080–5087

Contents lists available at ScienceDirect

Polymer

journal homepage: www.elsevier.com/locate/polymer

Preparation of polymer latex particles carrying salt-responsive fluorescent graft chains

Masakatsu Kasuya, Tatsuo Taniguchi*, Michinari Kohri, Keiki Kishikawa, Takayuki Nakahira

Division of Applied Chemistry and Biotechnology, Graduate School of Engineering, Chiba University, 1-33 Yayoi-cho, Inage-ku, Chiba 263-8522, Japan

ARTICLE INFO

Article history:
Received 16 April 2014
Received in revised form
8 August 2014
Accepted 10 August 2014
Available online 19 August 2014

Keywords:
Stimuli-responsive fluorescent polymer latex particle
Surface-initiated atom transfer radical polymerization
Copper-catalyzed azide-alkyne cycloaddition

ABSTRACT

We prepared the novel fluorescent polymer latex particles which can change their fluorescence intensity in response to the increasing NaCl concentration in water. Core polymer latex particles were synthesized by emulsifier-free emulsion polymerization of styrene and 2-(2-chloroisobutyroyloxy)ethyl methacrylate. Hydrophilic polymer chains containing epoxy groups were grafted from the core particles by surface-initiated atom transfer radical copolymerization of methoxy polyethyleneglycol methacrylate (MEO_xMA, $x = 4$ or 9) and glycidyl methacrylate in aqueous media. After azidation of epoxy groups in graft chains, a water-soluble fluorescent dansyl derivative was successfully coupled with the graft chains by copper-catalyzed azide-alkyne cycloaddition in aqueous media. The wavelength of maximum fluorescence intensity of polymer particles carrying graft chains with longer PEG side chains ($x = 9$) was slightly blue-shifted (7 nm) and the fluorescence intensity increased (1.35 times) with an increase in NaCl concentration as opposed to polymer particles with shorter PEG chains ($x = 4$).

1. Introduction

Polymer particles with a precisely controlled size, shape and chemical structure have attracted much attention over the past decade as smart materials responding to applied external stimuli such as temperature [1–6], pH [3–6], sugar [5,7,8], protein [9–11], magnetic field [12–19] and so on. Fluorescent polymer particles have immense potentials in biochemical applications because of the high efficiency and selectivity of fluorescence emission. For instance, quantum dots-containing polymer particles have been widely studied as a useful emission probe for bio-imaging and sensor technology due to a high absorption coefficient, a high fluorescence quantum yield, and photo-stability. Feng et al. developed an imaging system by co-encapsulation quantum dots and iron oxides in poly(lactic acid)-D-alpha-tocopheryl polyethylene glycol 1000 succinate nanoparticles [20]. Organic fluorescent dye-embedded polymer particles have been also studied energetically for biomedical applications including intracellular delivery, optical imaging and sensors. Larpent et al. prepared dual fluorescent polymer nanoparticles with a sensitive fluorescein-based dye on the surface and a reference dye entrapped within polystyrene-based core particles for ratiometric sensors [21].

For further functionalization of polymer particles, surface modification is quite effective because of a large specific surface area of nanoparticles compared to that of bulk materials. Surface modification techniques of solid substrates, such as grafting-from Refs. [10,22–26] or grafting-to method [26–28], layer-by-layer assembly [29–32], and click chemistry [31–35] have been actively developed. Grafting-from methods have been mainly conducted by surface-initiated controlled/living radical polymerization (CRP) like atom transfer radical polymerization (ATRP) [22–24,26], reversible addition fragmentation chain transfer (RAFT) polymerization [10,25], and initiator-transfer agent-terminator (iniferter) polymerization [27]. Among them, surface-initiated ATRP is regarded as the most useful technique for functionalization of particle surface because polymer chains can be grafted more densely than grafting-to technique. In addition to grafting-from methods, click chemistry including copper-catalyzed azide-alkyne cycloaddition (CuAAC) and thiol-ene reaction are also considered as a powerful technique for surface functionalization of various substrates because of their high efficiency, selectivity, and adaptability in aqueous media [36–40]. As functional molecules can be covalently attached to the surface of substrates, materials with precisely controlled chemical structure can be readily produced by click chemistry. Krueger et al.

* Corresponding author. Tel.: +81 43 290 3409.
E-mail address: taniguchi@faculty.chiba-u.jp (T. Taniguchi).

http://dx.doi.org/10.1016/j.polymer.2014.08.030
0032-3861/

demonstrated that fluorescent dyes can be covalently attached on the surface of diamond nanoparticles by CuAAC [41].

Polymer particles carrying fluorescence dyes on their surface are expected to respond sensitively to the environmental changes like ion concentrations, pH, temperature, solvent polarity, etc. Kawaguchi et al. investigated dependence of fluorescence on temperature and solvent compositions for dansyl-labeled core–shell and core-hair type microspheres [42]. By far, fluorescent polymer particles are potent substrates for biochemical applications, fluorescent polymer particles with a controlled architecture that respond to external stimuli have been not reported enough.

In our previous works on preparation of functional core–shell particles, the graft chain length (or shell thickness) on core particles was found to have enormous influence on physicochemical property [43–48] as well as the colloidal characteristics. Therefore, the particular attentions have been paid to the grafting-from technique by ATRP for controlled polymerization on polymer latex particles. In addition, the biocompatible PEG-based polymer chains with reactive sites grafted on latex particles have been regarded as the potential dispersed materials for practical applications in biomedical fields. Few studies on transformation of $PMEO_xMA$ graft chains carrying reactive sites on latex particles, however, have ever been reported in the literature to our knowledge. It would be of great interest to investigate the response of $PMEO_xMA$ chains grafted on particles to external stimuli such as salt concentration, temperature, and so on.

In this paper, we have represented that salt responsive fluorescent polymer latex particles with a novel architecture, the water-soluble fluorescent dansyl derivative was covalently attached to hydrophilic polymer chains grafted on the surface of polymer particles (Scheme 1).

Core polymer particles containing ATRP initiators were prepared by emulsifier-free emulsion polymerization of styrene (St) and 2-(2-chloroisobutyroyloxy)ethyl methacrylate (CiBM), and surface modification of the polymer particles was conducted by surface-initiated activator generated electron transfer atom transfer radical copolymerization (SI AGET-ATRP) of methoxy oligoethylene glycol methacrylate (MEO_xMA, $x = 4$ or 9) and glycidyl methacrylate (GMA). The reactive epoxy side-chains of graft polymers were then converted to the azide groups by a reaction with NaN_3. The water-soluble fluorescent dye, potassium 3-((5-(dimethylamino)-*N*-(prop-2-yn-1-yl)naphthalene)-1-sulfonamido)propane-1-sulfonate (Dansyl-anion), which was newly synthesized, was coupled with azide groups by CuAAC in aqueous media. The dispersion stability of the obtained polymer particles was examined in terms of the critical coagulation concentrations (CCCs). The dependence of emission behavior on NaCl concentration in aqueous dispersion was investigated by fluorescence spectrum measurement.

2. Experimental

2.1. Materials

St was obtained from Kanto Chemical and dried over calcium hydride and distilled under reduced pressure. Glycidyl methacrylate purchased from Kanto Chemical and methoxy polyethyleneglycol 400 methacrylate (MEO_9MA) kindly provided by Shin-Nakamura Chemical were passed through a basic alumina column to remove a polymerization inhibitor. Tris(2-pyridylmethyl)amine (TPMA) [49] and 5-(dimethylamino)-*N*-(prop-2-yn-1-yl)naphthalene-1-sulfonamide (Dansyl-alkyne) [50] were synthesized according to the methods reported in previous literatures. Thionyl chloride, methacryloyl chloride, tetraethyleleneglycol monomethyl ether, sodium azide, and pentamethyldiethylenetriamine (PMDETA) purchased from Wako Pure Chemical Industries were used as received. 2-Hydroxyisobutyric acid and potassium *tert*-butoxide were purchased from Tokyo Chemical Industry and used as received. 2-Hydroxyethyl methacrylate, triethylamine (TEA), 1,3-propanesultone, potassium persulfate (KPS), ethyleneglycol, cupper sulfate pentahydrate, copper chloride dehydrate, L(+)-ascorbic acid (AscA), sodium ascorbate

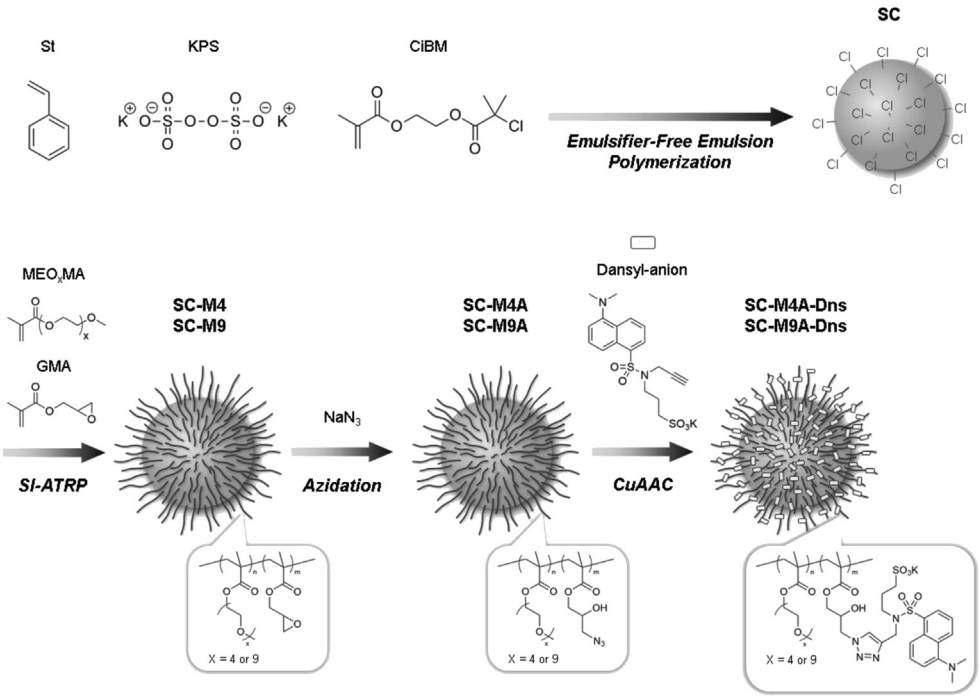

Scheme 1. Schematic protocol of preparation of salt-responsive polymer latex particles.

(NaAsc), and sodium chloride obtained from Kanto Chemical were used without further purification. The synthetic protocols of 2-chloroisobutyryl chloride, 2-hydroxyethyl 2-chloroisobutyrate (HCiB), 2-chloroisobutyroyloxyethyl methacrylate (CiBM), potassium 3-((5-(dimethylamino)-*N*-(prop-2-yn-1-yl)naphthalene)-1-sulfonamido)propane-1-sulfonate (Dansyl-anion) are described in Supporting Information. Deionized water with a resistance of 18.2 MΩ was obtained by passed through Millipore Simplicity UV system. Any other solvents were used as received.

2.2. Instruments

^{1}H and ^{13}C NMR spectra were measured by a JEOL Lambda 500 MHz Fourier transform NMR spectrometer. ESI-MS spectra were recorded on a Thermo Scientific Exactive mass spectrometer. FTIR spectra were obtained using a Jasco FTIR-420 spectrophotometer. Fluorescence spectra were measured by a HITACHI F-4010 spectrophotometer at 25 °C. UV-vis spectra were recorded on a HITACHI U-3010 spectrophotometer. Scanning electron microscopy (SEM) micrographs were obtained using a JEOL JSM-6510 operating at 20 kV. The zeta potentials in 10 mM NaCl aqueous solutions and the size distributions of polymer particles were measured by an Otsuka Electronics ELSZ-1000ZSCK zeta-potential and particle size analyzer. The average molecular weights of polymers were measured by size exclusion chromatography (SEC) using a Shodex SB804-HQ column with a Na_2HPO_4 (50 mM)/acetonitrile = 7/3 (v/v) mixed solvent as an eluent at a flow rate of 0.40 mL/min at 40 °C. The calibration curve was obtained by using poly(ethylene oxide) as a standard.

2.3. Synthesis of polymer latex particles bearing ATRP initiators

Polymer latex particles bearing ATRP initiators were synthesized by emulsifier-free emulsion polymerization. Into a three-necked round bottom flask equipped with a mechanical stirrer and a condenser, St (3.54 g, 34 mmol), KPS (0.135 g, 0.50 mmol), and deionized water (102 g) were charged and the suspension was deoxygenized by purging with argon for 15 min with stirring. The polymerization was started by heating to 70 °C in a water bath. After 4 h, CiBM (0.40 g, 1.7 mmol) bearing an ATRP initiating chlorine group was added to the suspension by a syringe and the reaction mixture was kept at 70 °C for additional 6 h. The suspension was cooled in an ice bath to stop polymerization, and filtered by passing through with a mesh filter. The obtained P(St-CiBM) particles were purified with a hollow fiber dialyzer using Spectrum Laboratories Pecyrum membrane (615 cm^2, 0.05 μm in a hollow diameter) connected to a Cole-Parmer Instrument Master Flex L/S tubing pump system to remove unreacted monomers and initiators. The solid contents were calculated using the weights of latex particles before and after freeze-drying.

2.4. Graft copolymerization on polymer latex particles by SI AGET-ATRP

MEO_9MA (2.53 g, 5.4 mmol), GMA (0.085 g, 0.60 mmol), $CuCl_2 \cdot 2H_2O$ (2.6 mg, 15 μmol), TPMA (6.5 mg, 22.5 μmol), and HCiB (2.5 mg, 15 μmol) were added to the aqueous dispersions of P(St-CiBM) polymer particles (30 mL, 1.0 wt%). The suspension was deoxygenized by purging with Ar for 15 min at 30 °C in a water bath. To this suspension was added an aqueous solution of AscA (0.10 mL, 3 mM), to begin graft polymerization. After 1 h, the graft polymerization was stopped by exposing the mixture to the air, and the suspension was centrifuged. The obtained supernatant was filtered and concentrated for GPC measurement. The grafted polymer particles were purified by four cycles of centrifugation and redispersion method to remove monomers, catalysts and free polymers adsorbed on the surface of polymer particles.

The graft copolymerization of MEO_4MA and GMA were carried out by applying the same protocol as for graft copolymerization of MEO_9MA and GMA by surface-initiated AGET ATRP except for using a monomer MEO_4MA (1.49 g, 5.4 mmol).

2.5. Azidation of epoxy side-chains of graft polymer

The polymer latex particles containing epoxy groups in their graft chains were diluted to 0.50 wt% with deionized water. To this 50 g suspension was added sodium azide (0.081 g, 1.25 mmol), and the suspension was heated at 50 °C in a water bath for 96 h. The resulting polymer particles were purified by two cycles of centrifugation and redispersion using an aqueous ammonia solution and by two cycles using a NaCl (10 mM) solution.

2.6. Introduction of dansyl derivatives to the graft polymer chains by CuAAC

Dansyl-anion (0.025 g, 0.055 mmol) was charged into the suspension of polymer particles (1.0 wt%, 19.2 g) containing azide groups in their graft polymer chains. An aqueous NaAsc solution (0.40 mL, 125 mM) was added to the suspension, followed by addition of aqueous $CuSO_4$/PMDETA solution (0.40 mL, 125 mM). The mixture was kept at 30 °C in a water bath for 96 h. The obtained dansyl-coupled polymer particles were purified by cycles of centrifugation and redispersion technique with an aqueous ammonia solution, methanol and deionized water to remove Dansyl-anion and catalysts adsorbed on the surface of polymer particles until fluorescence of aqueous supernatant derived from Dansyl-anion was disappeared.

2.7. Measurement of critical coagulation concentrations

An aqueous NaCl solution (5 mL), ranging from 10 mM to 5.0 M, was mixed with the dispersion of polymer particles (0.003 wt%), and stirred for one day at room temperature. The absorbance of the mixtures was measured in the wavelength from 600 to 400 nm. The slope of the double logarithmic plot of absorbance against wavelength, the so-called *n*-value [51], was plotted against the NaCl concentration to determine the critical coagulation concentrations (CCCs).

2.8. Measurement of fluorescence spectra of polymer particles in aqueous NaCl solutions

The dispersion of polymer particles (0.40 wt%, 1 mL) was added to an aqueous NaCl solution (1 mL) whose concentration range was from 10 mM to 5.0 M. The mixture was stirred for one day, and its fluorescence was measured by a fluorescence spectrophotometer (excited at 336 nm).

3. Results and discussion

3.1. Synthesis of polymer particles carrying ATRP initiators

Polymer latex particles bearing ATRP initiators were first synthesized by emulsifier-free emulsion polymerization of St and 2-(2-bromoisobutyroyloxy)ethyl methacrylate (BiBM) using KPS. Since polymer particles obtained were not dissolved unexpectedly in any common organic solvents such as tetrahydrofuran and chloroform, the content of BiBM in polymer particles could not be determined by ^{1}H NMR spectrum measurement. This may be attributed to homolytic cleavage of the active bromine–carbon bond of BiBM

during the emulsifier-free emulsion polymerization process, resulting in cross-linked structure of polymer particles. Therefore, CiBM with a less active halogen–carbon (chlorine–carbon) bond [52,53] was used as a monomer containing an ATRP initiating tertiary chlorine ester group. Polymer latex particles bearing ATRP initiators (abbreviated as SC) were then synthesized by emulsifier-free emulsion polymerization of St and CiBM using KPS. CiBM was copolymerized by a shot addition technique which has been known as a useful technique for surface-functionalization of polymer latex particles. The SEM image of SC core particles obtained is shown in Fig. S1 (a). The conversion of St was determined to be 85% by gravimetric method.

The copolymerized amount of CiBM was calculated by ^{1}H NMR spectrum measurement as reported in our previous paper [55]. Fig. 1(a) shows the ^{1}H NMR spectra of SC core particles dissolved in $CDCl_3$. The signals appeared at 6.2–7.5 ppm are assignable to aromatic protons (5H) of St units. When the integral values of aromatic protons are given as S_A, the integral value for one proton of St unit ($S_{1H\ St}$) corresponds to $S_A/5$. Accordingly, the integral value of CiBM protons per one proton ($S_{1H\ CiBM}$) can be calculated by eqs. (1) and (2) using the integral values (S_B) at 0.2–4.5 ppm arisen from the main chain protons (3H) of St units and all protons (15H) ascribed to CiBM units.

$$S_{1H\ CiBM} = (S_B - 3S_{1H\ St})/5 \quad (1)$$

$$C_{CiBM}(\text{mol\%}) = (S_{1H\ CiBM})/(S_{1H\ St}) \times 100 = (100 \times S_B/S_A) - 20 \quad (2)$$

The total amounts of copolymerized CiBM (C_{CiBM}) in SC particles was then determined to be 5.9 mol% with respect to St units by comparing the values between $S_{1H\ CiBM}$ and $S_{1H\ St}$. The amount of CiBM copolymerized in SC polymer particles is slightly larger than that of CiBM loaded in reaction media (5.0 mol% with respect to St). This may be caused by a faster polymerization rate of CiBM relative to that of styrene.

The hydrodynamic diameter of SC was measured to be 406 nm by DLS as shown in Fig. 2. The surface ATRP initiator density is one of the most important colloidal properties of grafted polymer particles. In general, the density of surface ATRP initiating groups

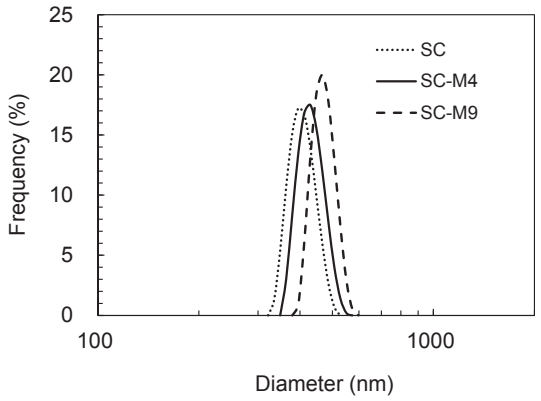

Fig. 2. Particle size distributions of SC (dotted line), SC-M4 (solid line), and SC-M9 (dashed line) polymer particles dispersed in water at 25 °C measured by DLS.

can be suitably measured by conductometric titration [54] or fluorescence technique [55]. The ATRP initiating group density at the surface of anionic SC particles was measured to be 0.11 groups/nm^2 by conductometric titration.

3.2. Surface-initiated AGET ATRP of MEO_xMA and GMA

The hydrophilic polymer chains containing reactive epoxy groups were grafted by surface-initiated AGET ATRP of MEO_xMA ($x = 4$ or 9) and GMA in aqueous media. TPMA was used as a ligand to suppress disproportionation of copper chloride in water [56]. HCiB was also used as a sacrifice free initiator to control graft copolymerizations and to investigate molecular weights of free polymers. The grafted polymer particles are abbreviated as SC-M4 and SC-M9 by using the number (x) of ethylene oxide repeating units in MEO_xMA.

As shown in Fig. 2, the particle size of SC-M4 and SC-M9 was measured to be 432 and 472 nm in water, respectively. SEM images of SC-M4 and SC-M9 dried particles are shown in Fig. S1 (b) and (c). The volume average diameters of SC-M4 and SC-M9 determined by SEM observation are 418 and 423 nm, respectively. The reason why

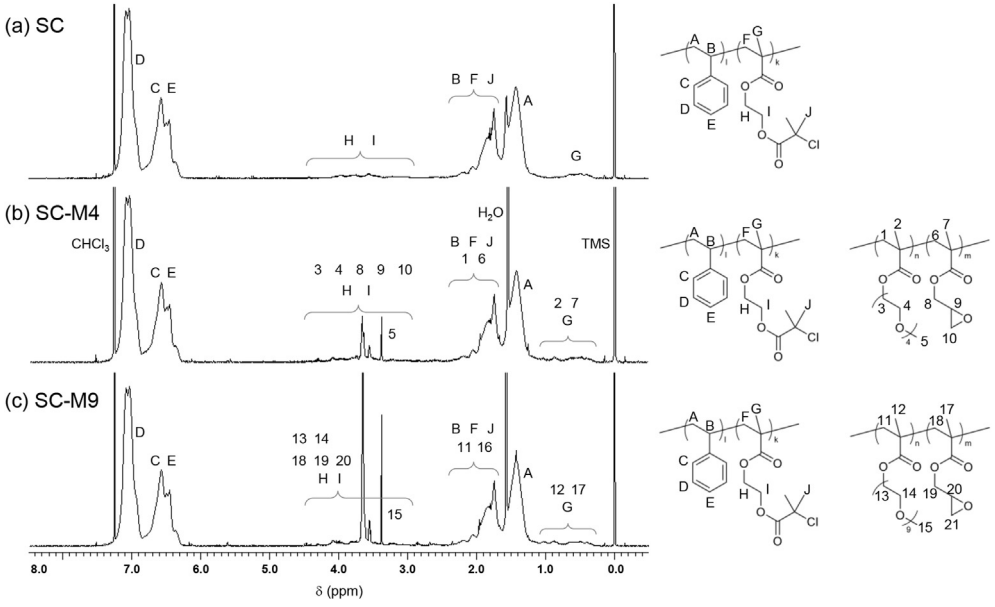

Fig. 1. ^{1}H NMR spectra of SC (a), SC-M4 (b) and SC-M9 (c) in $CDCl_3$ at r.t.

the volume average diameters measured by DLS are larger than those by SEM is that the hydrophilic graft chains of SC-M4 and SC-M9 particles are highly swollen in aqueous media.

GPC analysis revealed that the number average molecular weights of the free P(MEO_4MA-GMA) and P(MEO_9MA-GMA) were 27,300 (M_w/M_n = 1.47) and 41,900 (M_w/M_n = 1.62) for SC-M4 and SC-M9, respectively (GPC curves of free P(MEO_4MA-GMA) and P(MEO_9MA-GMA) are shown in Fig. S2). The amounts of GMA copolymerized into P(MEO_4MA-GMA) and P(MEO_9MA-GMA) were measured to be 20 and 18 mol%, respectively, by ^{1}H NMR spectra (Fig. S3), indicating that GMA more than a feed concentration (10 mol%) was copolymerized into graft chains. This may be due to the difference in polymerizability between smaller GMA and larger MEO_xMA. Considering the molecular weights as measured by GPC, the repeating numbers of MEO_4MA and GMA of free P(MEO_4MA-GMA) can be determined to be 88 and 22, respectively. Similarly, those of MEO_9MA and GMA of free P(MEO_9MA-GMA) can be estimated to be 84 and 19, respectively. Tsujii et al. reported that the molecular weights and the molecular weight distributions of free polymers are in good agreement with those of grafted polymers [57]. The graft densities of SC-M4 and SC-M9 were thus calculated to be 0.10 and 0.08 chains/nm^2, respectively, under the assumption that the composition of graft polymers are equal to that of free polymers. In order to examine the adequacy of the results obtained, the SC2 core and the SC2-M9 grafted particles were re-synthesized under same protocols as SC and SC-M9. The surface densities of ATRP initiators on SC2 and graft chains on SC2-M9 were estimated to be 0.10 groups/nm^2 and 0.07 chains/nm^2, respectively. These are in good agreement with results obtained for SC and SC-M9.

3.3. Fluorescent labeling of graft chains with dansyl-anion by CuAAC

Dansyl-anion was Dansyl-anion was coupled with graft polymer chains by azidation of epoxy groups and successive CuAAC in aqueous media. Azidation of reactive epoxy side-chains on graft polymers was conducted in an aqueous NaN_3 solution (50 mM) at 50 °C. The CuAAC coupling reaction with Dansyl-anion (2.5 mM) was carried out at 30 °C for more than 96 h in the presence of $CuSO_4$ and PMDETA (2.5 mM) as a catalyst and a ligand, respectively. The azidated particles and Dansyl-anion coupled particles are abbreviated as SC-M4A, SC-M9A, SC-M4A-Dns, and SC-M9A-Dns, respectively.

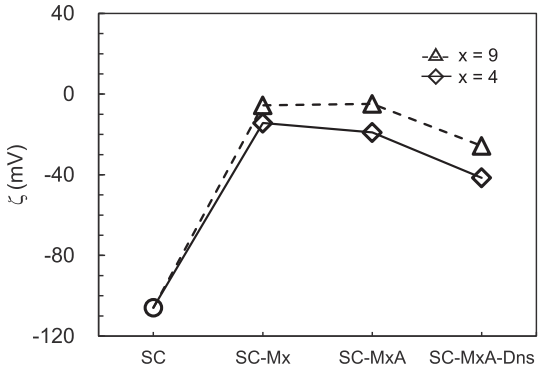

Fig. 4. Zeta potentials of SC (open circle), SC-M4, SC-M4A, SC-M4ADns (open diamond), SC-M9, SC-M9A-Dns, SC-M9A-Dns (open triangle) Particles in aqueous NaCl solutions (10 mM) at 25 °C.

Fig. 3 represents the FTIR spectra of a series of SC-M4 and SC-M9. The absorption band at 2100 cm^{-1}, assignable to azide groups of both SC-M4A and SC-M9A, was observed after azidation of SC-M4 and SC-M9. Additionally, the absorption was found to disappear completely after the CuAAC coupling reaction. These results support that both azidation and the consecutive CuAAC coupling reaction proceeded successfully. The hydrodynamic diameters of Dansyl-anion coupled SC-M4A-Dns (427 nm) and SC-M9A-Dns (477 nm) (Fig. S4) were almost equal to those of SC-M4 (432 nm) and SC-M9 (470 nm), suggesting that polymer particles remains their dispersion state stably during the above sequential reaction process. The SEM images of SC-M4A-Dns and SC-M9A-Dns particles are shown in Fig. S1 (d) and (e). The volume average diameters for SC-M4A-Dns and SC-M9-Dns were measured to be 416 and 425 nm, respectively.

The zeta potentials of SC, SC-M4, SC-M9, SC-M4A-Dns, and SC-M9A-Dns particles are summarized in Fig. 4. The zeta potentials of SC-M4 and SC-M9 were measured to be −14 and −6 mV, respectively. Given that the zeta potential of SC core particles is −106 mV, the graft chains bearing hydrophilic PEG side chains are considered to suppress the surface charges of core particles. In addition, the zeta potentials of particle are found to remain constant before and after azidation. It is worth noting that the zeta potentials of dansyl-coupled SC-M4A-Dns and SC-M9A-Dns particles decrease to −42 and −26 mV, respectively. These results support that Dansyl-anion is successfully linked to azidated graft chains by the CuAAC click reaction.

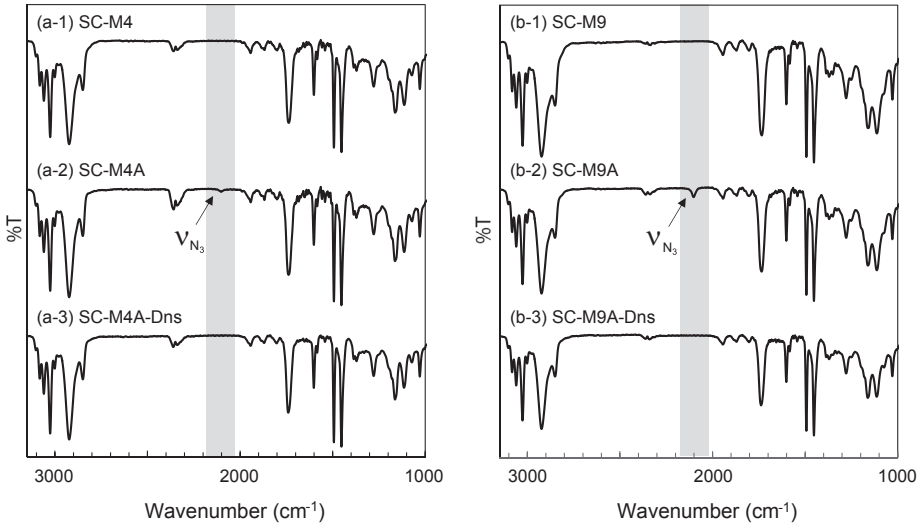

Fig. 3. FTIR spectra of SC-M4 (a-1), SC-M4A (a-2) and SC-M4A-Dns (a-3), SC-M9 (b-1), SC-M9A (b-2) and SC-M9A-Dns (b-3) polymer particles in KBr pellets.

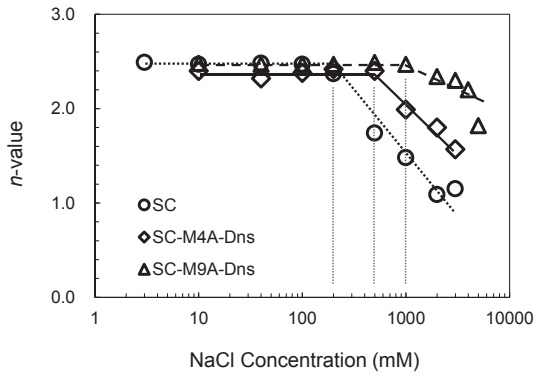

Fig. 5. Plots of *n*-value as a function of NaCl concentration for SC (open circle), SC-M4A-Dns (open diamond), and SC-M9A-Dns (open triangle) polymer particles.

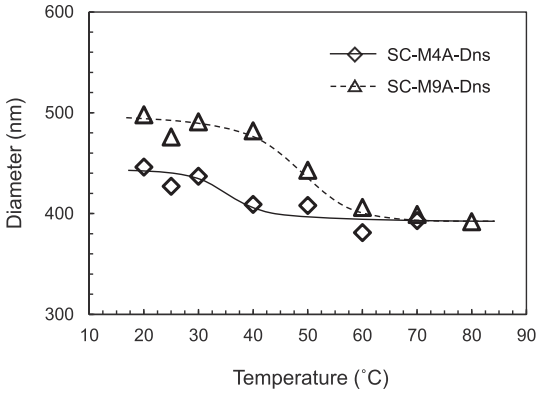

Fig. 7. Dependence of hydrodynamic diameters of SC-M4A-Dns (open diamond) and SC-M9A-Dns (open triangle) on temperature in water measured by DLS.

3.4. Critical coagulation concentrations

As the hydrophilic graft polymer chains are expected to improve the colloidal stability of polymer latex particles, the dispersion stability of SC, SC-M4A-Dns, and SC-M9A-Dns was compared in terms of critical coagulation concentrations (CCCs) of added NaCl.

Fig. 5 shows the plot of *n*-values against NaCl concentrations for SC, SC-M4A-Dns, and SC-M9A-Dns. Since the CCCs are defined as the electrolyte concentrations where *n*-values begin to decrease, CCCs for SC, SC-M4A-Dns, and SC-M9A-Dns were determined to be 200, 500, and 1000 mM, respectively. These results indicate that grafted polymer particles have a better dispersion stability due to the steric repulsions between the highly hydrated grafted chains on particles. The reason why the CCC of SC-M9A-Dns was larger than that of SC-M4A-Dns might be attributed to both the high graft density and the longer PEG side-chains of grafted polymer chains. It should be noted that *n*-values of SC-M9A-Dns decreased gradually than those of SC and SC-M4A-Dns in the NaCl concentration range over CCCs. SC-M9A-Dns particles are assumed to aggregate gradually with a progression of slow dehydration of longer PEG side chains compared to SC-M4A-Dns with a short PEG chain.

3.5. Quantification of amount of Dansy-anion linked to graft chains

In order to estimate the amount of conjugated Dansyl-anion, fluorescence spectra of SC-M4-Dns and SC-M9A-Dns dissolved in a THF/methanol (95/5, v/v) mixed solvent were compared with the standard samples prepared from Dansyl-anion dissolved in the same solvent. Since there was a slight difference in the maximum fluorescence emission wavelength (λ_{max}) between the coupled (508 nm) and the free (513 nm) Dansyl-anion, the amount of Dansyl-anion covalently-bonded to graft chains were calculated to be 3.6 and 11.3 groups/chains for SC-M4A-Dns and SC-M9A-Dns polymer particles, respectively, by comparing the fluorescence intensities at $\lambda = 508$ nm.

Since P(MEO_9MA-GMA) on SC-M9A-Dns possess hydrophilic long PEG side-chains, the graft chains might be highly swollen in water (Fig. 6 (a)). Therefore, azidation of epoxy groups on P(MEO_9MA-GMA) with azide ions was expected to proceed effectively. On the other hand, hydrophobic P(MEO_4MA-GMA) grafted on SC-M4A-Dns is considered to shrink their chains on particle surfaces (Fig. 6 (b)), resulting in less azidation of epoxy groups in aqueous media.

In order to examine the effect of PEG side chain length (x) upon the thermo-responsive property of graft chains on SC-M4A-Dns and SC-M9A-Dns particles, the cloud points of free P(MEO_xMA-GMA) were compared. As shown in Fig. S5, the cloud points of P(MEO_4MA-GMA) and P(MEO_9MA-GMA) were determined to be 51 and 76 °C, respectively. This indicates that SC-M4A-Dns particles with longer PEG side chains are considered to transform their graft chains easily with increase in temperature as compared with SC-M9A-Dns. In fact, there is a difference in transition temperatures from a swollen to a shrunk sate between SC-M4A-Dns and SC-M9A-Dns as shown in Fig. 7.

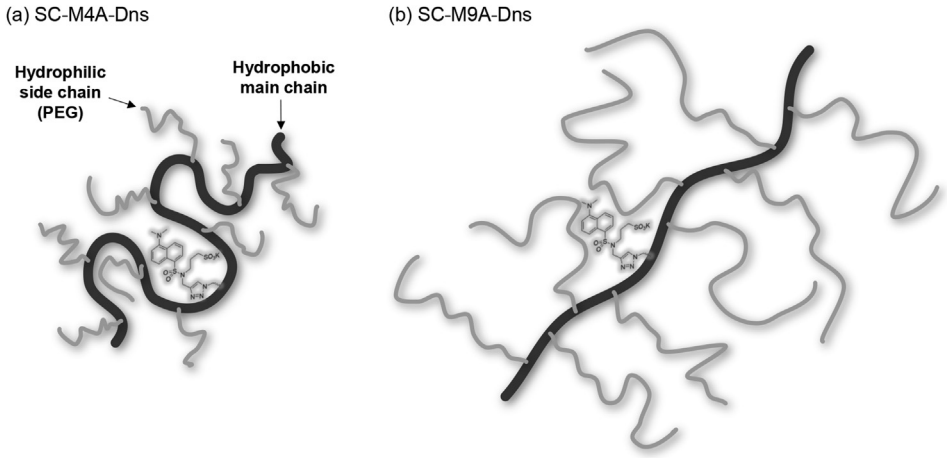

Fig. 6. Expected microscopic structure of graft chains for SC-M4A-Dns (a) and SC-M9A-Dns (b) in water.

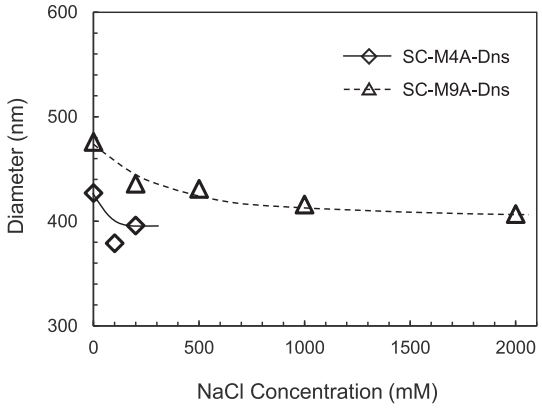

Fig. 8. Dependence of hydrodynamic diameters of SC-M4A-Dns (open diamond) and SC-M9A-Dns (open triangle) on NaCl concentration measured by DLS at 25 °C.

There is the same tendency among P(MEO$_x$MA-GMA) to decrease their size in response to addition of NaCl. Whereas SC-M4A-Dns particles drastically collapse their graft chains and approach to almost the same size of SC core particles by a slight increase in NaCl concentration (<200 mM), SC-M9A-Dns particles gradually decrease their shell thickness over a range of 2000 mM as shown in Fig. 8. The above results are qualitatively consisted with the results of random copolymer of MEO$_x$MA and methacrylic acid as reported by Stöver [58].

3.6. Emission behavior of dansyl-modified polymer particles dispersed in aqueous media

The hydrated state of graft chains is considered to affect the microscopic environment around Dansyl-anion covalently linked to polymer chains. Thus, the fluorescence emission behavior of Dansyl-anion in PEG400/water mixtures was first investigated. Fluorescence spectra of Dansyl-anion are shown in Fig. S6. Fig. S7 shows that the fluorescence intensities increase monotonically with an increase in a PEG400 volume ratio and become 24 times larger in 99.9 vol% of PEG400 than that in pure water. In addition, a significant blue-shift of λ_{max} (from 558 nm to 526 nm) was observed with increasing the volume ratio of PEG400 in a mixture.

Fluorescence spectra of SC-M4A-Dns and SC-M9A-Dns dispersed in NaCl aqueous solutions are shown in Figs. S8 and S9, respectively. Fig. 9 represents the effect of NaCl concentration on λ_{max} of SC-M4A-Dns and SC-M9A-Dns. SC-M9A-Dns was found to have longer λ_{max} compared to SC-M4A-Dns, suggesting that

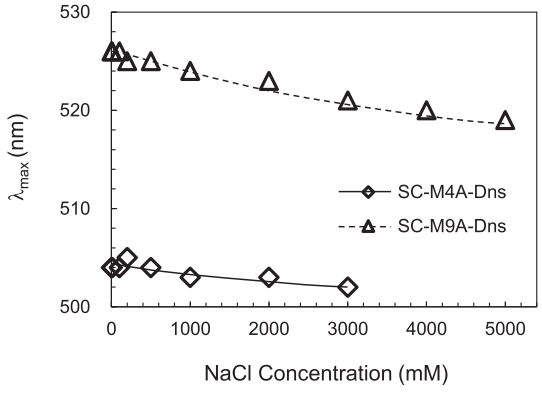

Fig. 9. Effect of NaCl concentration on λ_{max} of SC-M4A-Dns (open diamond) and SC-M9A-Dns (open triangle).

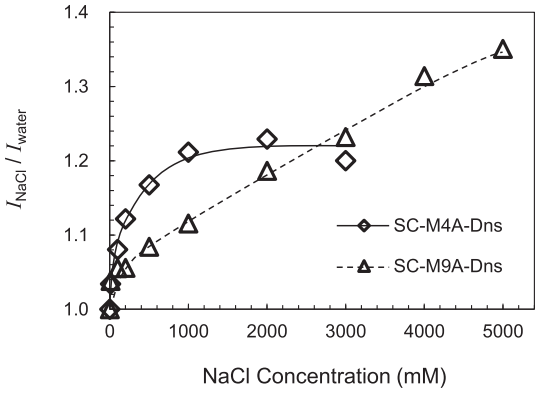

Fig. 10. Effect of NaCl concentration on I_{NaCl}/I_{water} of SC-M4A-Dns (open diamond) and SC-M9A-Dns (open triangle).

Dansyl-anion groups conjugated in SC-M9A-Dns are situated mainly in a polar aqueous phase. These indicate that dansyl moieties in SC-M4A-Dns are much influenced by a hydrophobic character of particle surfaces and the main chains of grafted polymers when compared to SC-M9A-Dns. According to the previous literatures, the polar environment of Dansyl-anion in SC-M4A-Dns and SC-M9A-Dns corresponds approximately to ethyl acetate and tetrahydrofuran (λ_{max} = 509 nm). It should be noted that the larger variation in λ_{max} of SC-M9A-Dns (from 526 nm to 519 nm) reflects the gradual dehydration of a longer PEG side chain over the entire range of NaCl concentration above CCC. By contrast, a decrease in λ_{max} of SC-M4A-Dns (from 504 nm to 502 nm) by addition of a small amount of NaCl indicates that the shorter PEG side chains sensitively transform their conformation to a tightly shrunk state compared to the longer ones. Based on the above results of the CCCs, the changes in hydrodynamic diameter, and the emission behavior, the successive progression of dehydration of graft chains and aggregation of particles in response to NaCl addition might be summarized as follows. The graft chains are first dehydrated by addition of NaCl, leading to a decrease in hydrodynamic diameter of particles, as shown in Fig. 8. In general, latex particles are known to become less stable and form loose aggregates as the electrolyte concentration is increased to CCC (Fig. 5). Further addition of NaCl over CCC results in tightly collapse of graft chains due to the intensive dehydration as shown in Fig. 9.

The emission intensities of SC-M4A-Dns and SC-M9A-Dns in NaCl aqueous solutions relative to those in pure water, namely I_{NaCl}/I_{water}, are plotted in Fig. 10. I_{NaCl}/I_{water} of SC-M4A-Dns shows a rapid rise with an increase in NaCl concentration and reached a plateau (1.22) when the NaCl concentration is 1000 mM or more. On the other hand, I_{NaCl}/I_{water} of SC-M9A-Dns gradually increases to 1.35 at 3000 mM of NaCl concentration far beyond of CCC. These results support that the difference in simultaneous or gradual dehydration of PEG side chain between SC-D4A-Dns and SC-D9A-Dns in response to the increasing NaCl concentration as discussed above.

4. Conclusions

In this study, the salt-responsive emission behavior of dansyl-labeled polymer chains grafted on latex particles was successfully demonstrated. The polymer particles possessing the fluorescent dansyl-derivative on their graft chains were prepared by a combination of surface-initiated AGET ATRP, azidation of epoxy groups, and CuAAC of Dansyl-anion in aqueous media. The graft polymer chains with hydrated PEG side chains were found to increase the dispersion stability compared to before grafting. The wavelength of

maximum fluorescence intensity (λ_{max}) of SC-M9A-Dns decreased from 526 nm to 519 nm and the relative emission intensity (I_{NaCl}/I_{water}) increased 1.35 times with increasing NaCl concentration in contrast to SC-M4A-Dns. The novel technique proposed in this study is expected as a potential procedure to prepare stimuli-responsive polymer particles applicable in various fields such as biomedical materials, photo-imaging sensors, and so on.

Acknowledgment

The authors acknowledge Shin-Nakamura Chemical for providing some of the reagents.

Appendix A. Supplementary data

Supplementary data related to this article can be found online at http://dx.doi.org/10.1016/j.polymer.2014.08.030.

References

[1] Xiao X-C, Chu L-Y, Chen W-M, Wang S, Li Y. Adv Funct Mater 2003;13:847–51. http://dx.doi.org/10.1002/adfm.200304513.
[2] Suzuki D, Tsujii S, Kawaguchi H. Chem Lett 2005;34:242–3. http://dx.doi.org/10.1246/cl.2005.242.
[3] Chuang C-Y, Don T-M, Chiu W-Y. J Polym Sci A Polym Chem 2009;47:2798–810. http://dx.doi.org/10.1002/pola.23369.
[4] Cui K, Zhu D, Cui W, Lu X, Lu Q. J Phys Chem C 2012;116:6077–82. http://dx.doi.org/10.1021/jp.211847b.
[5] Wang Y, Zhang X, Mu J, Li C. New J Chem 2013;37:796–803. http://dx.doi.org/10.1039/c2nj40998d.
[6] Alam MA, Rabbi MA, Miah MAJ, Rahman MM, Ahmad H. J Colloid Sci Biotechnol 2012;1:225–34. http://dx.doi.org/10.1166/jcsb.2012.1019.
[7] Zenkl G, Mayr T, Klimant I. Macromol Biosci 2008;8:146–52. http://dx.doi.org/10.1002/mabi.200700174.
[8] Zenkl G, Klimant I. Macrochim Acta 2009;166:123–31. http://dx.doi.org/10.1007/s00604-009-0172-0.
[9] Diehl C, Schlaad H. Chem Eur J 2009;15:11469–72. http://dx.doi.org/10.1002/chem.200901420.
[10] Ugajin H, Oka N, Okamoto T, Kawaguchi H. Colloid Polym Sci 2013;291:109–15. http://dx.doi.org/10.1007/s00396-012-2685-z.
[11] Pfaff A, Barner L, Müller AHE, Granville AM. Eur Polym J 2011;47:805–15. http://dx.doi.org/10.1016/j.eurpolymj.2010.09.020.
[12] Medeiros SF, Santos AM, Fessi H, Elaissari A. Int J Pharm 2011;403:139–61. http://dx.doi.org/10.1016/j.ijpharm.2010.10.011.
[13] Elaissari A. Macromol Symp 2009;281:14–9. http://dx.doi.org/10.1002/masy.200950702.
[14] Ruhland TM, Reichstein PM, Majewski AP, Walther A, Müller AHE. J Colloid Interface Sci 2012;374:45–53. http://dx.doi.org/10.1016/j.jcis.2012.01.028.
[15] Kong SD, Sartor M, Hu C-MJ, Zhang W, Zhang L, Jin S. Acta Biomater 2013;9:5447–52. http://dx.doi.org/10.1016/j.actbio.2012.11.006.
[16] Yan S, Zhang X, Sun Y, Wang T, Chen X, Yin J. Colloids Surf B 2014;113:302–11. http://dx.doi.org/10.1016/j.colsurfb.2013.09.004.
[17] Medeiros SF, Santos AM, Fessi H, Elaissari A. J Colloid Sci Biotechnol 2012;1:99–112. http://dx.doi.org/10.1166/jcsb.2012.1002.
[18] Macková H, Horák D, Trachtová Š, Rittich B, Španová A. J Colloid Sci Biotechnol 2012;1:235–40. http://dx.doi.org/10.1166/jcsb.2012.1018.
[19] Medeiros SF, Lara BR, Oliveira PFM, Moraes RM, Alves GM, Elaissari A. J Colloid Sci Biotechnol 2013;2:180–94. http://dx.doi.org/10.1166/jcsb.2013.1052.
[20] Tan YF, Chandrasekharan P, Maity D, Yong CX, Chuang K-H, Zhao Y, et al. Biomaterials 2011;32:2969–78. http://dx.doi.org/10.1016/j.biomaterials.2010.12.055.
[21] Allard E, Larpent C. J Polym Sci A Polym Chem 2008;46:6206–13. http://dx.doi.org/10.1002/pola.22931.
[22] Cheesman BT, Neilson AJG, Willott JD, Webber GB, Edmondson S, Wanless EJ. Langmuir 2013;29:6131–40. http://dx.doi.org/10.1021/la4004092.
[23] Lu X, Jiang R, Fan Q, Zhang L, Zhang H, Yang M, et al. J Mater Chem 2012;22:6965–73. http://dx.doi.org/10.1039/c2jm15768c.
[24] Min K, Hu J, Wang C, Elaissari A. J Polym Sci A Polym Chem 2002;40:892–900. http://dx.doi.org/10.1002/pola.10160.
[25] Xu S, Li J, Chen L. J Mater Chem 2011;21:4346–51. http://dx.doi.org/10.1039/c0jm03593a.
[26] Berger S, Synytska A, Ionov L, Eichhorn K-J, Stamm M. Macromolecules 2008;41:9669–76. http://dx.doi.org/10.1021/ma802089h.
[27] Anraku Y, Takahashi Y, Kitano H, Hakari M. Colloids Surf B 2007;57:61–8. http://dx.doi.org/10.1016/j.colsurfb.2007.01.003.
[28] Han J, Kim H, Kim Y, Jo SM, Jang S-Y. ACS Nano 2010;4:3503–9. http://dx.doi.org/10.1021/nn100574g.
[29] Shi J, Du C, Shi J, Wang Y, Cao S. Macromol Biosci 2013;13:494–502. http://dx.doi.org/10.1002/mabi.201200411.
[30] Mauser T, Déjugnat C, Sukhorukov GB. Macromol Rapid Commun 2004;25:1781–5. http://dx.doi.org/10.1002/marc.200400331.
[31] Huang C-J, Hong C-W, Ko F-H, Chang F-C. Soft Matter 2011;7:10850–5. http://dx.doi.org/10.1039/c1sm06312j.
[32] Huang C-J, Chang F-C. Macromolecules 2009;42:5155–66. http://dx.doi.org/10.1021/ma900478n.
[33] Tedja R, Soeriyadi AH, Whittaker MR, Lim M, Marquis C, Boyer C, et al. Amal Rose 2012;3:2743–51. http://dx.doi.org/10.1039/c2py20450a.
[34] Goldmann AS, Barner L, Kaupp M, Vogt AP, Barner-Kowollik C. Prog Polym Sci 2012;37:975–84. http://dx.doi.org/10.1016/j.progpolymsci.2011.11.008.
[35] Álvarez-Paino M, Marcelo G, Muñoz-Bonilla A, Rodríguez-Hernández J, Fernández-García M. Polym Chem 2013;4:986–95. http://dx.doi.org/10.1039/c2py20824e.
[36] Goldmann AS, Walther A, Nebhani L, Joso R, Ernst D, Loos K, et al. Macromolecules 2009;42:3707–14. http://dx.doi.org/10.1021/ma900332d.
[37] Dördelmann G, Meinhardt T, Sowik T, Krueqer A, Schatzschneider U. Chem Commun 2012;48:11528–30. http://dx.doi.org/10.1039/C2CC36491C.
[38] Patel KG, Swartz JR. Bioconjugate Chem 2011;22:376–87. http://dx.doi.org/10.1021/bc100367u.
[39] Hayashi K, Ono K, Suzuki H, Sawada M, Moriya M, Sakamoto W, et al. Chem Mater 2010;22:3768–72. http://dx.doi.org/10.1021/cm100810g.
[40] Gu W, Chen G, Stenzel MH. J Polym Sci A Polym Chem 2009;15:5550–6. http://dx.doi.org/10.1002/pola.23615.
[41] Meinhardt T, Lang D, Dill H, Krueger A. Adv Funct Mater 2011;21:494–500. http://dx.doi.org/10.1002/adfm.201001219.
[42] Horie K, Yamada S, Machida S, Takahashi S, Isono Y, Kawaguchi H. Macromol Chem Phys 2003;204:131–8. http://dx.doi.org/10.1002/macp.200290064.
[43] Taniguchi T, Kashiwakura T, Inada T, Kunisada Y, Kasuya M, Kohri M, et al. J Colloid Interface Sci 2010;347:62–8. http://dx.doi.org/10.1016/j.jcis.2010.03.019.
[44] Taniguchi T, Inada T, Kashiwakura T, Murakami F, Kohri M, Nakahira T. Colloids Surf A Physicochem Eng Aspects 2011;377:63–9. http://dx.doi.org/10.1016/j.colsurfa.2010.12.026.
[45] Taniguchi T, Obi S, Kamata Y, Kashiwakura T, Kasuya M, Ogawa T, et al. J Colloid Interface Sci 2012;368:107–14. http://dx.doi.org/10.1016/j.jcis.2011.11.077.
[46] Taniguchi T, Murakami F, Kasuya M, Kojima T, Kohri M, Saito K, et al. Colloid Polym Sci 2013;291:215–22. http://dx.doi.org/10.1007/s00396-012-2658-2.
[47] Taniguchi T, Kasuya M, Kunisada Y, Miyai T, Nagasawa H, Nakahira T. Colloids Surf B Biointerf 2009;71:194–9. http://dx.doi.org/10.1016/j.colsurfb.2009.02.010.
[48] Kohri M, Sato M, Abo F, Inada T, Kasuya M, Taniguchi T, et al. Eur Polym J 2011;47:2351–60. http://dx.doi.org/10.1016/j.eurpolymj.2011.09.016.
[49] Tyeklár Z, Jacobson RR, Wei N, Murthy NN, Zubieta J, Karlin KD. J Am Chem Soc 1993;115:2677–89. http://dx.doi.org/10.1021/ja00060a017.
[50] Bolletta F, Fabbri D, Lombardo M, Prodi L, Trombini C, Zaccheroni N. Organometallics 1996;15:2415–7. http://dx.doi.org/10.1021/om950793b.
[51] Long JA, Osmond DW, Vincent B. J Colloid Interface Sci 1973;42:545–53.
[52] Andrieux CP, Gallardo I, Savéant J-M, Su K-B. J Am Chem Soc 1986;108:638–47. http://dx.doi.org/10.1021/ja00264a013.
[53] Tang W, Kwak Y, Braunecker W, Tsarevsky NV, Coote ML, Matyjaszewski K. J Am Chem Soc 2008;130:10702–13. http://dx.doi.org/10.1021/ja802290a.
[54] Jayachandran KN, Takacs-Cox A, Brooks DE. Macromolecules 2002;35:4247–57. http://dx.doi.org/10.1021/ma011651y.
[55] Kasuya M, Taniguchi T, Motokawa R, Kohri M, Kishikawa K, Nakahira T. J Polym Sci A Polym Chem 2013;51:4042–51. http://dx.doi.org/10.1002/pola.26800.
[56] Tsarevsky NV, Matyjaszewski K. Chem Rev 2007;107:2270–99. http://dx.doi.org/10.1021/cr050947p.
[57] Tsujii Y, Ohno K, Yamamoto S, Goto A, Fukuda T. Adv Polym Sci 2006;197:1–45. http://dx.doi.org/10.1007/12_063.
[58] Jones JA, Novo N, Flagler K, Pagnucco CD, Carew S, Cheong C, et al. J Polym Sci A Polym Chem 2005;43:6095–104. http://dx.doi.org/10.1002/pola.21099.